

# Preparation and Characterization of Al Matrix Composites Reinforced with (20-x) wt.-% Al<sub>2</sub>O<sub>3</sub> - (x) ZrO<sub>2</sub>

Mahmoud F. Zawrah <sup>a\*</sup>, Mohammed A. Taha <sup>b</sup>, F. A. Saadallah<sup>b</sup>, A.G. Mostafa<sup>c</sup>,  
M.Y. Hassan<sup>c</sup>, Mahmoud Nasr <sup>b</sup>

<sup>a</sup> Ceramics Department, National Research Center , Dokki, Cairo, Egypt.

<sup>b</sup> Solid State Physics Department, National Research Center, Dokki, Cairo, Egypt.

<sup>c</sup> Physics Department, Faculty of Science, Al-Azhar University, Nasr City, Cairo, Egypt.

## Abstract

Metal matrix nanocomposites composed of Al-(20-x) wt.-% Al<sub>2</sub>O<sub>3</sub> - (x) ZrO<sub>2</sub>, x=0, 1, 2 & 4, were prepared by mechanical alloying technique. The powders' mixture was milled in a planetary ball mill up to 7h. The effect of milling time on properties of obtained powders was studied by using X-ray diffraction analysis (XRD) and transmission electron microscopy (TEM) to investigate phase composition, crystal size and morphology of the milled powders. In order to study the sinterability, the milled nanocomposite powders were cold pressed and sintered in argon atmosphere at different firing temperatures i.e. 300, 370 and 470°C for 1h. Physical properties, namely, bulk density and apparent porosity of sintered bodies were determined by Archimedes method. Phase identification and microstructure of the sintered composites were investigated by using XRD and scanning electron microscope (SEM) as well as energy dispersive spectrometer (EDS). Microhardness of sintered composite was also examined using Vickers hardness indenter. The results were discussed in terms of the effect of milling time on the properties of the prepared powders and sintered composites. The results revealed that the grain size of milled powders was about 30 nm with a noticeable presence of agglomerates. Uniform distribution of nano-sized alumina-zirconia particles in the aluminum matrix could be achieved with increasing milling time. The density of the sintered composites was affected by milling time of starting powders and firing temperature. It increased with increasing milling time and firing temperature. Microhardness of sintered bodies was found to be progressively increased with increasing of milling time of starting powders.

**Key words:** metal-matrix composites (MMCs); mechanical properties; mechanical alloying

---

\*Corresponding author: M.F. Zawrah, National Research Center, Al-Behooth St., Cairo, Egypt, Email: [mzawrah@hotmail.com](mailto:mzawrah@hotmail.com), Fax: +20233370931.

## 1. Introduction

Owing to low density, low melting point, high specific strength, high hardness, high-specific elastic modulus and high thermal conductivity of aluminum, it has been used as engineering material in the aerospace, automobile industries, electric wires and sports machines [ **D.B. Miracle, D.B et al 2005; Torralba, G.M et al 2003; Woo. K et al 2007**]. A wide variety of reinforcement particulates such as SiC, B<sub>4</sub>C, Al<sub>2</sub>O<sub>3</sub>, ZrO<sub>2</sub>, AlN, Si<sub>3</sub>N<sub>4</sub>, TiC, TiO<sub>2</sub>, TiB<sub>2</sub> and graphite have been used to reinforce aluminum[**Fogognolo, J.B et al 2003**].

High energy ball milling is a simple and useful technique for attaining a homogeneous distribution of inert fine particles within a fine grained matrix [**Prabhu, B et al 2006; Cullity, B.D et al 2001; Estrada-Guel, I et al 2009**]. During ball milling, two essential processes occur, cold welding between the different particles and fracturing of cold welded particles due to high energy collision [**Lu, L et al 1999**]. The cold welding minimizes diffusion distance between atoms of different components. The fracturing of welded particles impedes the clustering of particles promoting transfer of high ball collision energy to all particles and produces new clean surfaces without the oxide layers accelerating diffusion [ **Lu, L et al 1999; Gubicza, J et al 2004; Rosenberger, M.R et al 2005**]. Reinforcing of ductile Al matrix with hard particles such as oxides provides a suitable combination of the properties of both phases which, in turn, results in an improvement of physical and mechanical properties of composites [ **Fogognolo, J.B et al 2003; Zebarjad, S.M et al 2006; Suryanarayana, C et al 2013; ; Zebarjad, S.M et al 2007**]. On the other hand, it has been shown that nano-crystalline matrices strengthened by nano-sized reinforcement are expected to have much better microstructural stabilities and performance than nano-crystalline materials [ **Fogognolo, J.B et al 2003**], because of the concurrence of strengthening by both grain boundary and nanoparticle reinforcements [ **Kaufman, J.G 2002; Khakbiz, M et al 2009; Liu, Y.Q et al 2009**]. Uniform dispersion of fine reinforcements and a fine grain size of the matrix contribute to improve the mechanical properties of the composite [**Khakbiz, M et al 2009; Hassan, S.F et al 2008**]. The main goal of this work is to investigate the effect of milling time on the properties of Al - (20-x) wt.-% Al<sub>2</sub>O<sub>3</sub> - (x) ZrO<sub>2</sub>, x=0, 1, 2 &4 composite powders and sintered bodies. The effect of milling time on the crystallite size, lattice strain, relative density, apparent porosity, microhardness, and morphological properties was considered.

## 2. Materials and Methods

Firstly, a mixture of Al and Al<sub>2</sub>O<sub>3</sub> powders with purities 99 & 98.2% and average particle sizes  $\geq 74$  &  $2\mu\text{m}$ , respectively, were transferred into the milling machine (Desktop high energy planetary ball mill, type MTI SFM-1 (QM - 3SP2)) to prepare Al-20wt.-%Al<sub>2</sub>O<sub>3</sub> nanocomposite at different milling times (1,3,5 and 7h). Stearic acid was also taken as process controlling agent to prevent agglomeration of the powder mixtures

during milling. The milling process conditions were: ZrO<sub>2</sub> and Al<sub>2</sub>O<sub>3</sub> balls with different diameters (6-20mm), 500 rpm rotating speed and 10:1 ball-to-powder weight ratio.

Secondly, in order to examine the properties enhancement of Al-Al<sub>2</sub>O<sub>3</sub> composite, different amounts of zirconia powder (1, 2 & 4 wt.-%, average particle size; 35 nm) was added on the starting mixture (Al - 20wt. % Al<sub>2</sub>O<sub>3</sub> at the expense of alumina and was milled for 7 h.

For the milled powder, X-ray diffraction data was collected at ambient temperature in step scanning mode using a computerized controlled X-ray diffractometer (PANalytical Empyrean, Netherlands) with Cu K<sub>α</sub>- radiation ( $\lambda$  K<sub>α</sub>= 1.5406 Å) operated at 30 mA and 45 kV. The powder diffraction pattern was scanned in 2 $\theta$  range of 20-80° with scan step 0.013 and counting time 20 s/step. The data obtained by XRD was used to calculate the crystallite size and lattice strain. Transmission electron microscope (TEM) type JEOL JEM-1230, operating at 120 kV and attached with a CCD camera, was employed to investigate the morphology and particle size of milled powders at different milling times.

The composite powder was compacted into small compacts of desired size at room temperature. Specimen of 10 mm diameter and 4 mm height were compacted in a hardened steel pre-compaction die set using hydraulic compressor at 10 MPa. The compacted samples were sintered at different temperatures i.e. 300, 370 and 470°C, in argon atmosphere for one hour and heating rate 8°C/min.

The relative density and apparent porosity of the sintered samples were determined by Archimedes method. Theoretical density of compacted samples was calculated using the simple rule of mixtures, considering the fully dense values of Al and Al<sub>2</sub>O<sub>3</sub> are 8.96 and 3.95 g/cm<sup>3</sup>, respectively. An optical imaging was performed for all samples in order to support the structural study. Optical microscope model OLYMPUS-BX51, equipped with digital DP12cam was used. Scanning electron microscope (SEM), attached with energy dispersive spectroscopy unit (EDX), model “Philips XL30” was also used to investigate the microstructure of sintered samples.

The reinforcement behavior of sintered composites was estimated by microhardness measurement (Vickers hardness machine-model: Shimadzu corporation hardness tester) by applying 1.961N load for 10 sec. during measuring hardness. The hardness value of the investigated materials was measured as average of 5 readings along the cross section surface of the specimens.

### **3. Results and Discussion**

#### **3.1. Characterization of the prepared powders**

##### **3.1.1 Phase composition of prepared powders**

XRD patterns of mechanically alloyed Al-20wt. % Al<sub>2</sub>O<sub>3</sub> composite milled for 1, 3, 5, and 7h are shown in Figure 1. The expected two phases Al and Al<sub>2</sub>O<sub>3</sub> are obtained and compared with the data in cards (88-0826&03-0932) [18-19][ Youssef, K.M et al 2006; Liu, R.S et al 1997. With increasing milling time, the peaks tend to get broadened

associated with weakens in their intensities. Similar results were reported for Al-Al<sub>2</sub>O<sub>3</sub> composite [ Moustafa, M.M et al 2013; Aboraia, M.S et al 2013].

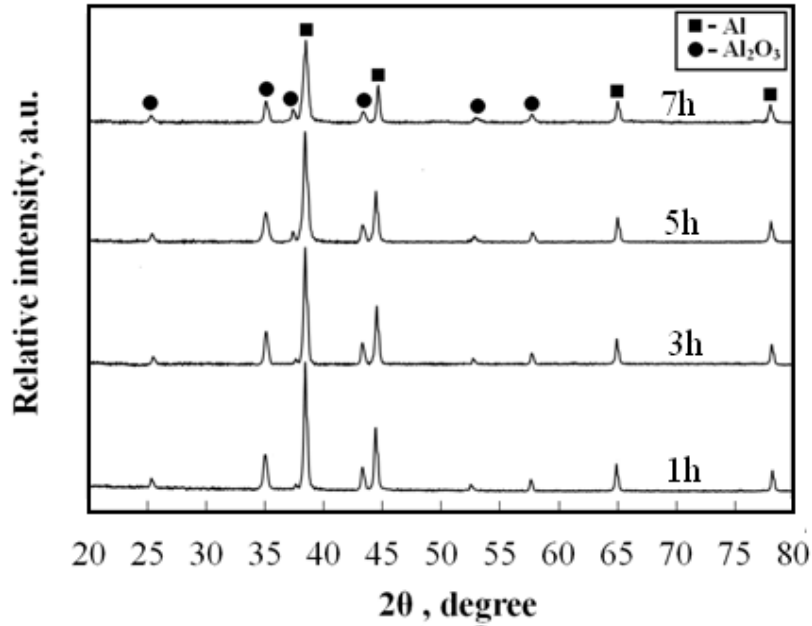


Fig. 1: XRD patterns of mechanically alloyed Al-20wt.-% Al<sub>2</sub>O<sub>3</sub> composites milled at 1, 3, 5, and 7h.

Fig. 2 shows full width at half maximum (FWHM) calculated from X-ray diffraction patterns for Al-20wt.-% Al<sub>2</sub>O<sub>3</sub> powders. The broadening in peaks with increasing milling time is due to the severe lattice distortion and grain size refinement [ **Rajkovic, V et al 2008; Lonnberg, B et al 1994** ] .

Fig. 3 depicts crystallite size and lattice strain of milled powders calculated from XRD peak broadening, versus milling time. It is indicated that the crystal size (D) decreases with increasing milling time (t) according to the equation:  $D=Kt^{-2}$ , where K is a constant [ **Tousi, S.S.R et al 2009; Suryanarayana, C 2001** ]. The reduction happened in Al crystal size and an elevated strain energy stored inside particles could be obtained because of the severe plastic deformation introduced during ball milling by hard Al<sub>2</sub>O<sub>3</sub> particles. It can be, in a part, attributed to hindering the dislocation movement by Orowan bowing mechanism, leading to an increase in the dislocation density thereby accelerating the crystal refining progress. Consequently, the lattice strain is found to be increased with increasing milling time (Fig.3). Similar results have been reported by many researches [ **Tousi, S.S.R et al 2009; Zhou, F et al 2001; Zhou, U et al 2006; Hesabi, Z.R et al 2006; Maurice, D et al 1995** ] . Oxidation of Al and formation of solid solution between metals and ceramics causes changes in the lattice parameters.

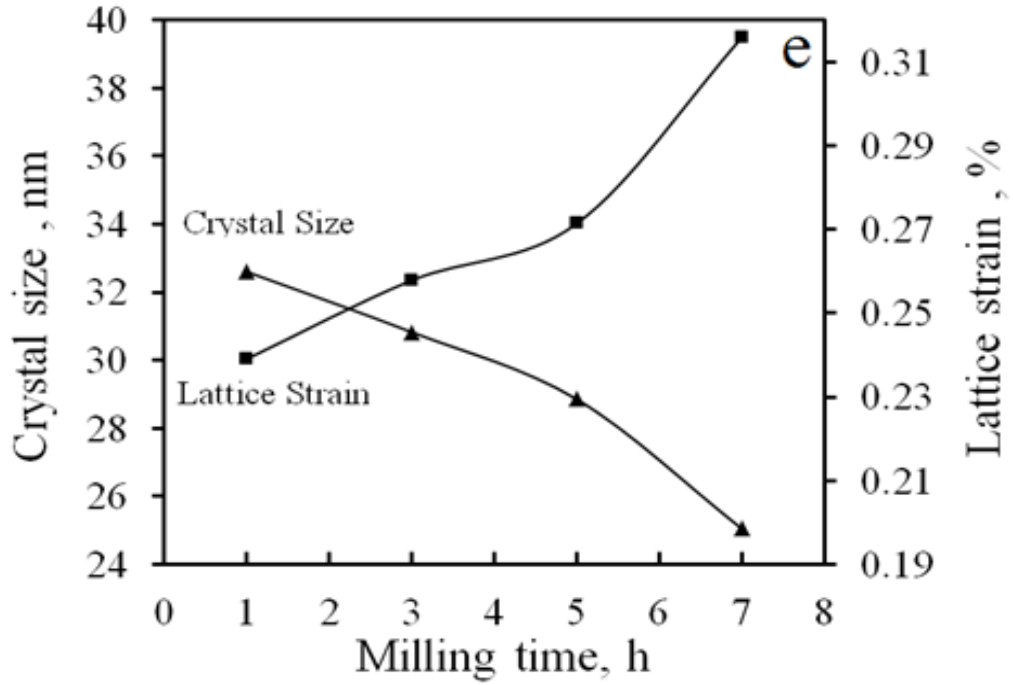


Fig. 2: Full width at half maximum (FWHM) of Al-20 wt. %  $\text{Al}_2\text{O}_3$  versus milling time.

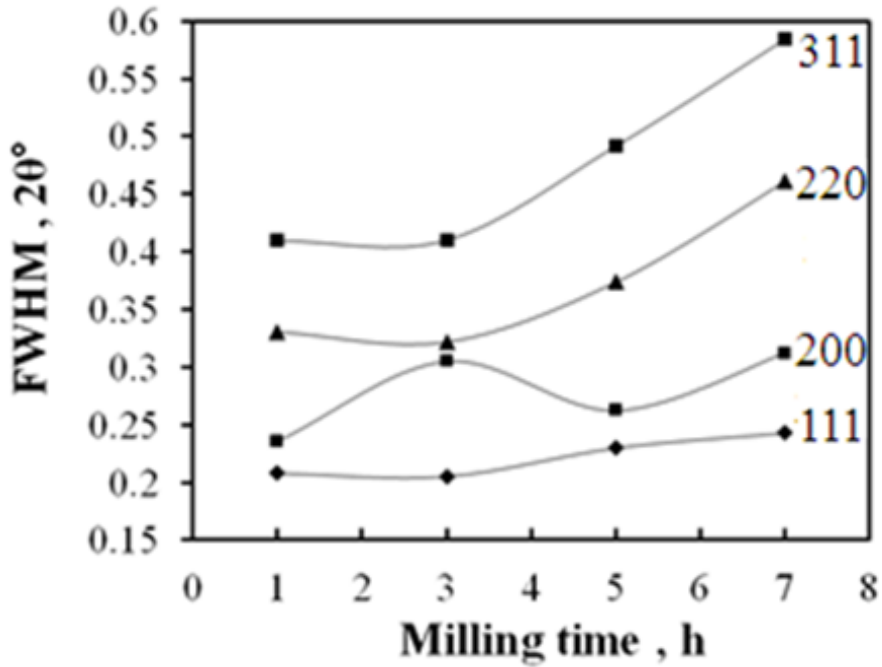


Fig. 3: Crystal size and lattice strain of Al-20 wt. %  $\text{Al}_2\text{O}_3$  milled at different milling times.

Fig.4 shows the relationship between lattice parameters calculated for the principle planes (h k l) i.e. 111, 200, 220 & 311, using obtained XRD data and milling time. The results obtained indicate that the lattice parameter remains constant with increasing milling time. This means that neither oxidation of Al nor formation of solid solution between Al and Al<sub>2</sub>O<sub>3</sub> has been took place.

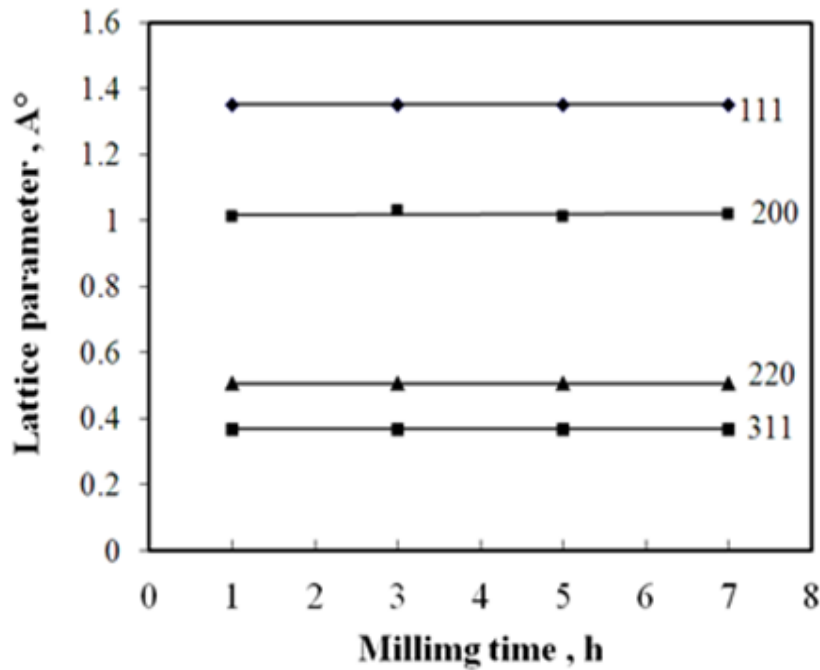


Fig. 5: XRD patterns of Al - (20-x) wt.-% Al<sub>2</sub>O<sub>3</sub> - (x) ZrO<sub>2</sub>, x=0, 1, 2 & 4 composites milled for 7 h.

Fig. 5 shows XRD of Al-(20-x) wt.-% Al<sub>2</sub>O<sub>3</sub> - (x) ZrO<sub>2</sub> composites containing 1, 2 and 4 wt.-% ZrO<sub>2</sub>. In case of addition 1 and 2 wt.-% zirconia, no new peaks beside Al and Al<sub>2</sub>O<sub>3</sub> are observed, but when the percentage increased to 4wt.-%, small peak related to zirconia (101) is detected at  $2\theta = 30.27^\circ$ , (X-ray card no. 88-1007) [ Francisco, A.T.G et al 2009; Zhao, Z et al 2005; Rao, P.G et al 2003] .

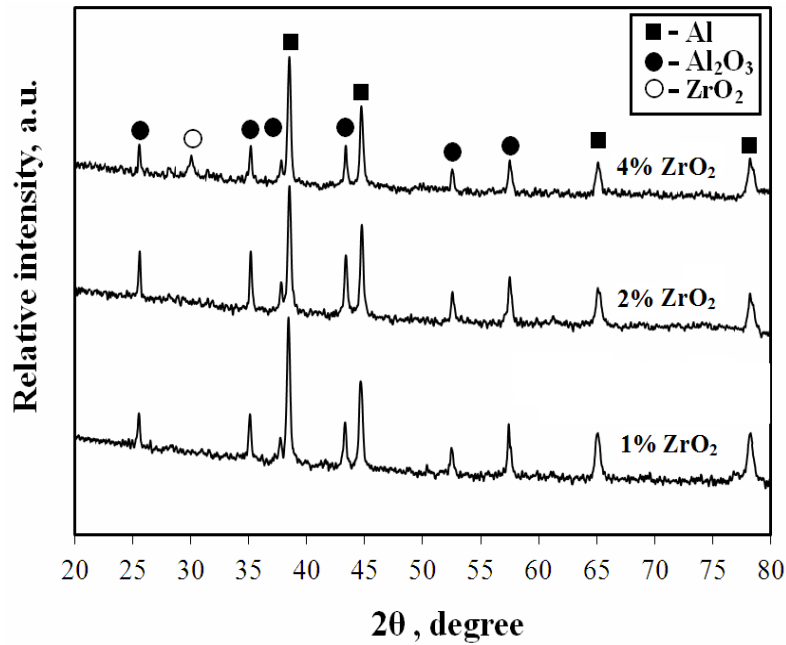


Fig. 5: XRD patterns of Al - (20-x) wt.-%  $\text{Al}_2\text{O}_3$  - (x)  $\text{ZrO}_2$ , x=0, 1, 2 & 4 composites milled for 7 h.

Fig. 6 shows relationship between lattice strain & crystal size versus zirconia's concentration. Decreasing in crystal size and increasing in lattice strain are indicated with increasing zirconia content. Beside the above mentioned reason, the decreasing in crystal size may be also related to the more hardened  $\text{ZrO}_2$  particles embedded in Al- $\text{Al}_2\text{O}_3$  matrix which cases more plastic deformation.

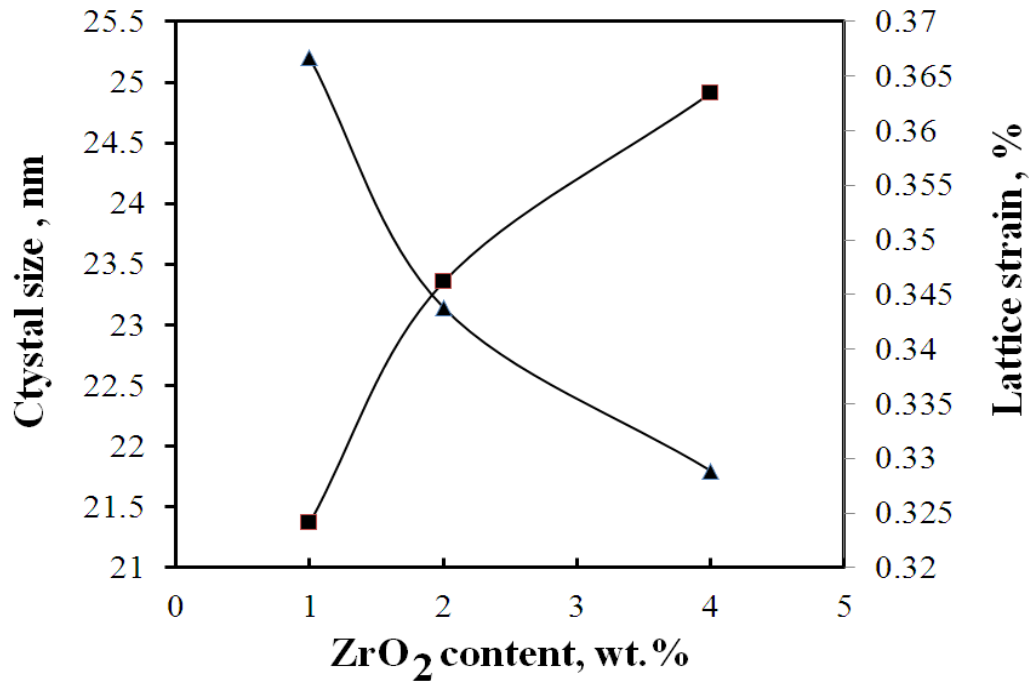


Fig. 6: Lattice strain and crystal size versus of Al - (20-x) wt.-% Al<sub>2</sub>O<sub>3</sub> - (x) ZrO<sub>2</sub>, x=0, 1, 2 & 4 composites.

### 3.1.2 Morphology of prepared powders

In order to investigate the morphology and particle size of the composite powder, transmission electron microscopy (TEM) was used. Fig.7 shows TEM images of Al-20wt. % Al<sub>2</sub>O<sub>3</sub> composite powder milled for 1, 3, 5, and 7hrs. As regards particle size, it is evident from TEM images that it decreases with increasing of milling time. After 1 and 3h milling, agglomerated alumina particles are extremely observed (Fig.7a & 7b). Such particles' agglomeration could be removed by increasing milling time. After 5h milling (Fig.7c), alumina agglomerates are also observed but they are smaller and less than that obtained after 1 and 3h milling. After 7h milling, it seems like a few amounts of alumina particles welded with aluminum matrix (Fig.7d). It is well known that at the first stage of milling, the ductile particles undergo deformation (plastic deformation) while brittle particles undergo fragmentation. Then, when ductile particles start to weld, the brittle particles come between two or more ductile particles at the instant of ball collision. However, no evidence of particle coarsening could be obtained through TEM. The raw powder of aluminum and alumina become continually intermixed leading to a homogenous material with a uniform second phase dispersion, i.e. alumina. This is because planetary mill is a high-energy mill which operates under high velocity and the



collision with milling balls enhances the powder refinement. During that, the powder particles are repeatedly deformed, cold welded and fractured by colliding balls. Fine and hard alumina particles are also act as milling agent, which help in reducing the powder [Fogognolo, J.B et al 2003; Rajkovic, V et al 2008; Tousi, S.S.R et al 2009] . In this situation, with more fracturing occurred, a large amount of fresh particle surfaces was produced. It is noted that finer alumina particle is distributed more homogeneously in MA composite. This is because mechanically alloying breaks up and continually embeds the alumina particles into aluminum matrix by repeated fracturing and cold welding of the powder charge [ Hussain, Z et al 2008]. The average particle size increases until the welding process dominates the milling process, and oppositely decreases after the fracture process becomes dominant. By achieving the balance between fracture and welding processes, the particles are rather uniform and equiaxed (i.e. no new changes) [ Maurice, D et al 1995, Rajković, V et al 2004] .

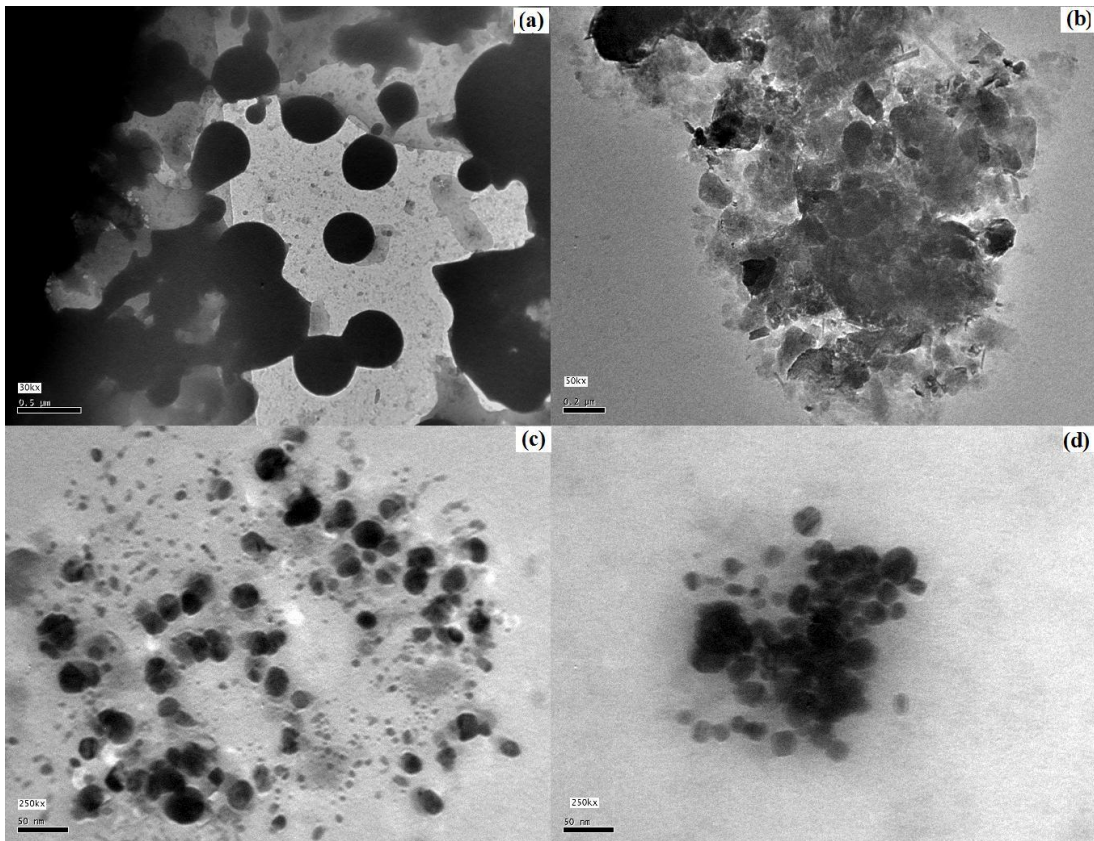


Fig. 7: TEM micrographs of Al-20 wt.-% Al<sub>2</sub>O<sub>3</sub> composites milled at, (a) 1h, (b) 3h, (c) 5h, and (d) 7 h.

Fig. 8 shows TEM image of  $ZrO_2$  powder, it used to enhance the properties of Al- $Al_2O_3$  composite matrix. the size of  $ZrO_2$  about 35 nm with sphere-like shape. Such shape is likely to produce more force agent on the other particles (i.e. Al and  $Al_2O_3$ ) and acting as milling balls in milling process and reaching by aluminum and alumina particles to smaller size in the whole mixture when added, specially 4 wt.-% (Fig. 9c). In fact, the more hardness the more behaving milling agent, the less hardness the less milling effect.

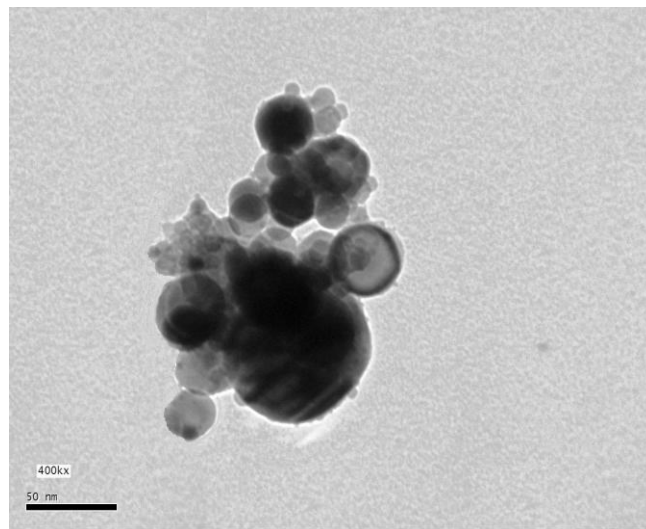
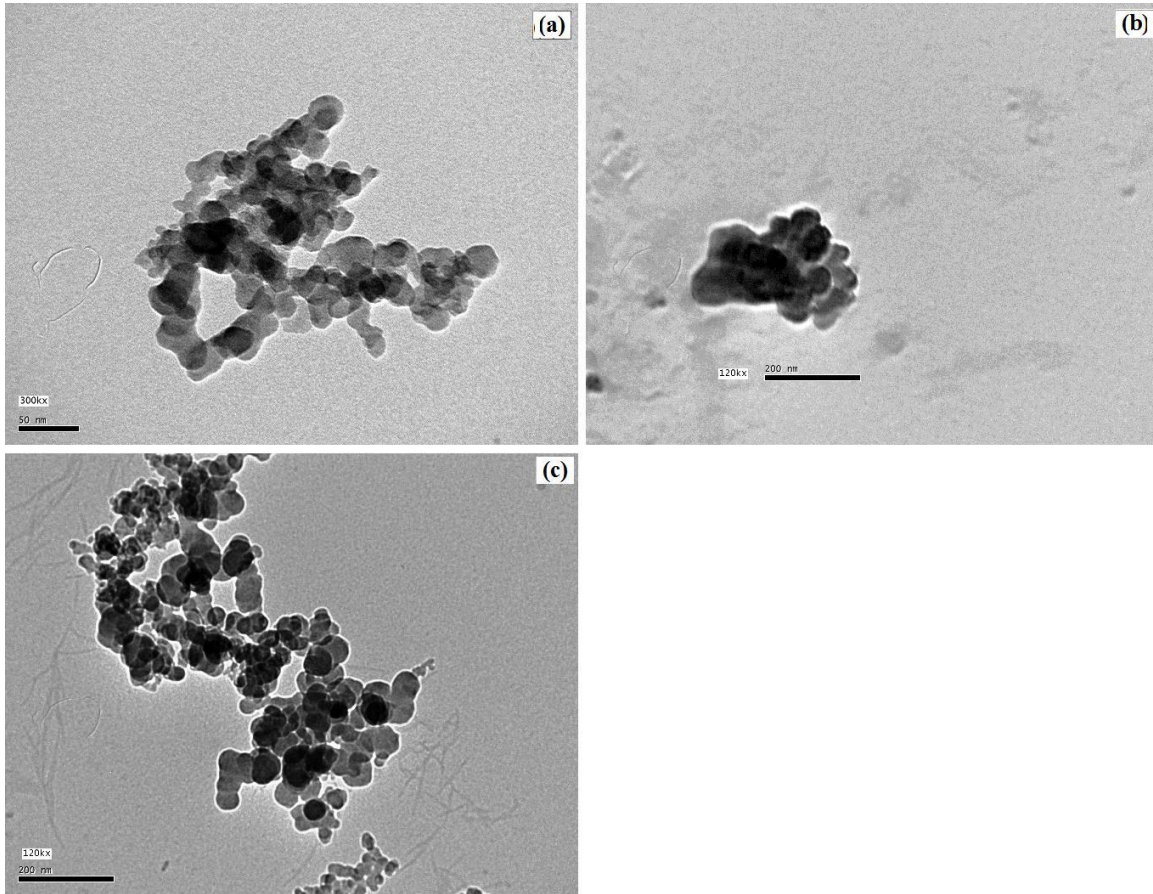


Fig. 8: TEM image of  $ZrO_2$  powder.

Fig. 9: TEM micrographs of Al - (20-x) wt.-% Al<sub>2</sub>O<sub>3</sub> - (x) ZrO<sub>2</sub>, x= 1, 2 & 4



composites milled for 7h.

## 3.2. Sintering of prepared nanocomposite powders

### 3.2.1. Relative density and apparent porosity

Fig. 10 shows the relative density and apparent porosity of Al-20wt.-% Al<sub>2</sub>O<sub>3</sub> nanocomposites sintered at different sintering temperatures i.e. 370, 400 and 470 °C, for 1 h in argon atmosphere. The relative density of sintered samples increases with increasing both milling time and sintering temperature. This is due to increasing of surface area and decreasing of particle sizes, reaching to nano scale, which associate with aluminum matrix and the reinforcement material “alumina” after milling for long time. In deeply interpretation, with increasing sintering temperature, the actions of complex diffusion mechanisms become more intense, directly affecting the formation of surface contacts between the particles forming closed pores and grain growth [ **Zawrah, M.F et al 2013; Korać, M et al 2007** ], are the matter causes the relative density increasing tendency. On the other hand, apparent porosity is found to be decreased with the increase in both milling time and sintering temperature (Fig.11). These results have been observed in many previous researches [ **Hanumanth, G.S et al 1993** ] .

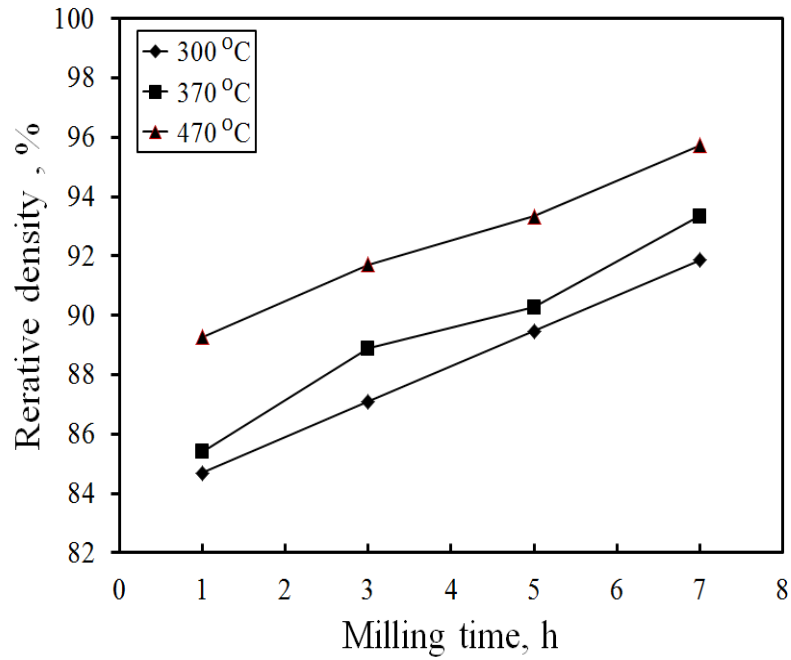
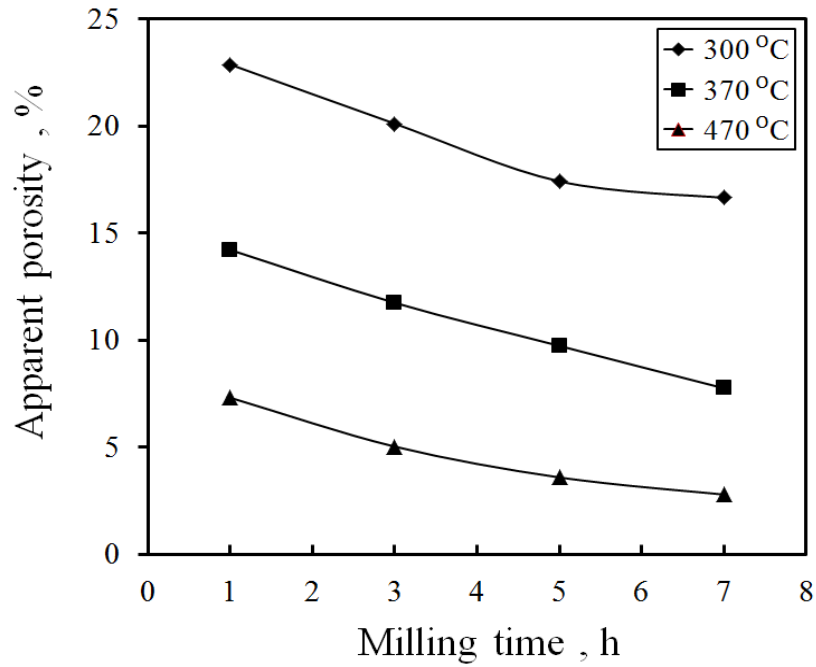


Fig. 10: Relative density vs. milling time for Al-20 wt. % Al<sub>2</sub>O<sub>3</sub> composites sintered at different temperatures



Apparent porosity vs. milling time for Al-20 wt. % Al<sub>2</sub>O<sub>3</sub> composites sintered at different temperatures.

Fig. 12 depicts the relative density and apparent porosity of Al - (20-x) wt.-% Al<sub>2</sub>O<sub>3</sub> - (x) ZrO<sub>2</sub> composites sintered at 470°C. It is indicated that the relative density increases with increasing ZrO<sub>2</sub> content. Also, the relative density of the composite containing ZrO<sub>2</sub> is higher than that of the composite without zirconia (Fig. 11). This is attributed to two factors; the first is the higher theoretical density of zirconia as compared to aluminum and alumina, while the second is the small size of zirconia which achieves more filling for the grain boundaries. Consequently, apparent porosity is found to be decreased from 27.5% to 23% with zirconia addition. Guimaraes et al. have been recorded similar results for Al<sub>2</sub>O<sub>3</sub>-ZrO<sub>2</sub> matrix [ Francisco, A.T.G et al 2009].

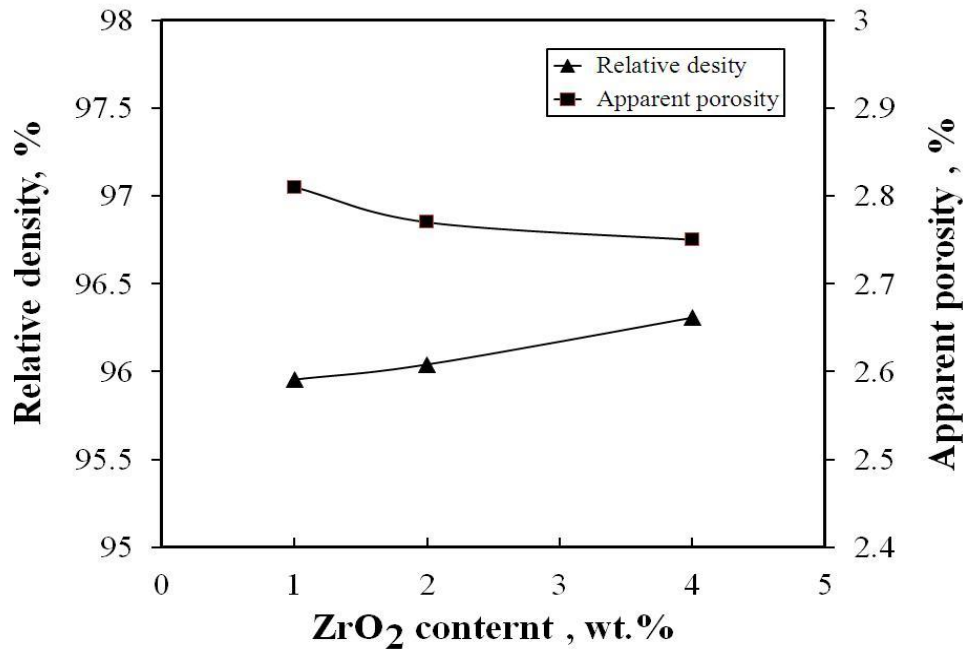


Fig. 12: Relative density and apparent porosity of Al - (20-x) wt.-% Al<sub>2</sub>O<sub>3</sub> - (x) ZrO<sub>2</sub>, x= 1, 2 & 4 composites milled for 7h and sintered at 470°C.

### 3.2.2. Microstructure of the sintered composites

Fig.13 shows optical micrographs of Al-20wt.-% Al<sub>2</sub>O<sub>3</sub> sintered in argon atmosphere at 470 °C for 1 h and prepared from powders milled at 1, 3, 5 and 7 hrs. A homogeneous microstructure with uniform distribution of alumina in the aluminum matrix is detected. Its homogeneity is increased with increasing milling time of starting



powders. The usage of mechanical alloying technique leads to obtain appreciable grain size reduction with increasing in milling time and less agglomerated regions.

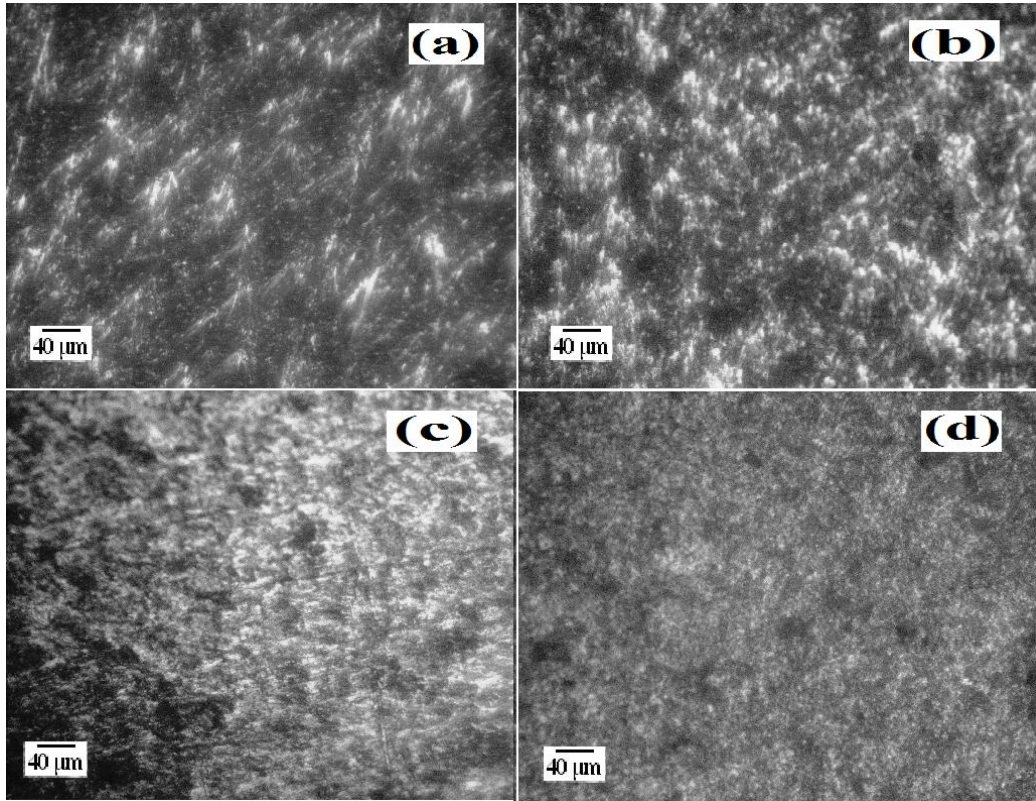


Fig. 13: Optical micrographs for Al-20 wt. %  $\text{Al}_2\text{O}_3$  composites sintered for 1 h at 470 °C in argon and prepared from powers milled at 1,3,5 and 7h.

For more details about the microstructure, SEM was conducted for Al-20 wt.-%  $\text{Al}_2\text{O}_3$  prepared form powder milled for 7hrs and sintered in argon atmosphere at 470 °C for 1h. Nearly homogeneous microstructure with good distribution of the reinforcement (alumina) is appeared in the image. Some agglomerated particle with grain growth is also detected in a dense microstructure. The particle agglomeration may cause by reduction of distances between the composite particles. Energy dispersive spectroscopy (EDX) area analysis of Al-20 wt.-%  $\text{Al}_2\text{O}_3$  composite prepared from powder milled for 7h and sintered at 470 °C for 1 h is shown in Fig. 15. Form the figure, it is indicated that the weight percent of Al and O are 71.51 and 28.49, respectively, which are corresponding to aluminum and alumina.

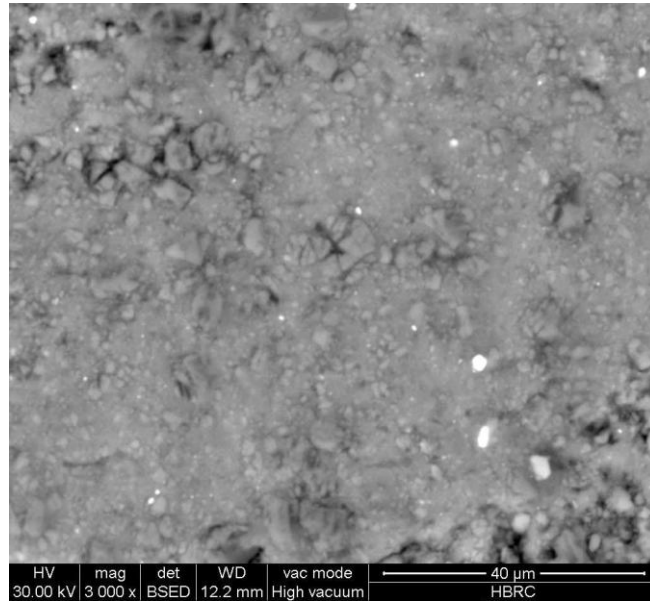


Fig. 14: SEM micrographs of Al-20 wt.-%  $\text{Al}_2\text{O}_3$  composite sintered for 1 h at  $470^\circ\text{C}$  prepared from powder milled for 7h.

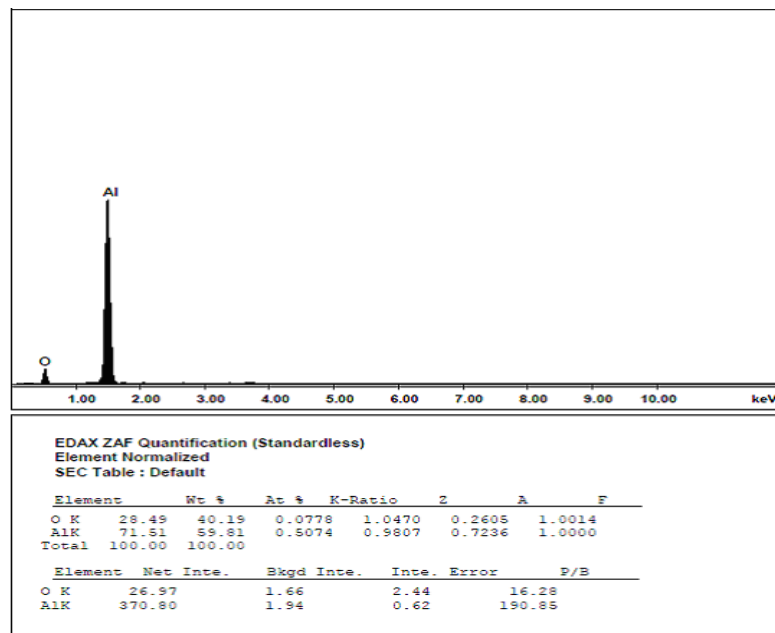


Fig. 15: EDAX of Al-20 wt.-%  $\text{Al}_2\text{O}_3$  composite sintered for 1 h at  $470^\circ\text{C}$  prepared from powder milled for 7h.

Fig.16 shows optical imaging of Al - (20-x) wt.-%  $\text{Al}_2\text{O}_3$  - (x)  $\text{ZrO}_2$ ; x= 1, 2 & 4, prepared from powder milled for 7 hrs and sintered in argon atmosphere at  $470^\circ\text{C}$  for 1h.

More fine and homogeneous microstructure is detected after addition of zirconia as compared that without zirconia.

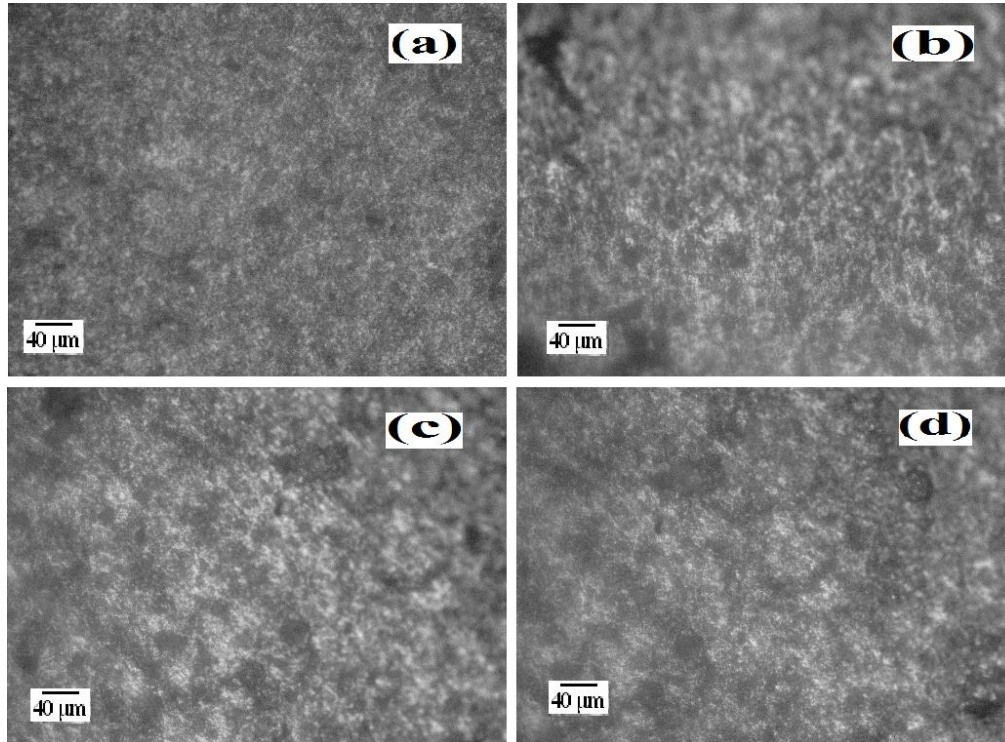


Fig. 16: Optical micrographs Al-(20-x)wt.-% Al<sub>2</sub>O<sub>3</sub>-(x)ZrO<sub>2</sub>, x=1, 2&4, composites sintered for 1 h at 470 °C in argon and prepared from powers milled for 7h.

Fig.17 show SEM micrograph of Al - (20-x) wt.-% Al<sub>2</sub>O<sub>3</sub> - (x) ZrO<sub>2</sub>; x=4, composite prepared from powder milled for 7h and sintered at 470 °C for 1 h. It is indicated from the image that more compacted, homogeneous and dense microstructure without grain growth is obtained. The porosity is mostly disappeared in this microstructure as compared that without zirconia. EDAX analysis shown in Fig. 18 indicates that the composite contains 71.98% Al, 24.79% O and 3.23% Zr.



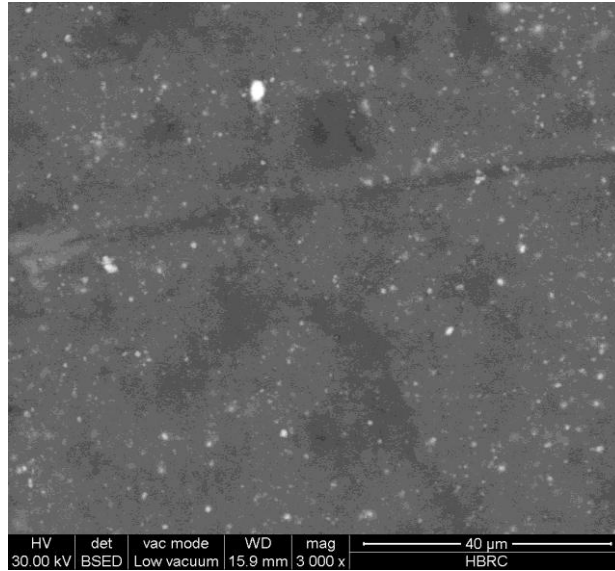


Fig. 17: SEM micrographs Al - (20-x) wt.-% Al<sub>2</sub>O<sub>3</sub> - (x) ZrO<sub>2</sub>, x= 4, composite sintered for 1 h at 470 °C in argon and prepared from powers milled at 7h.

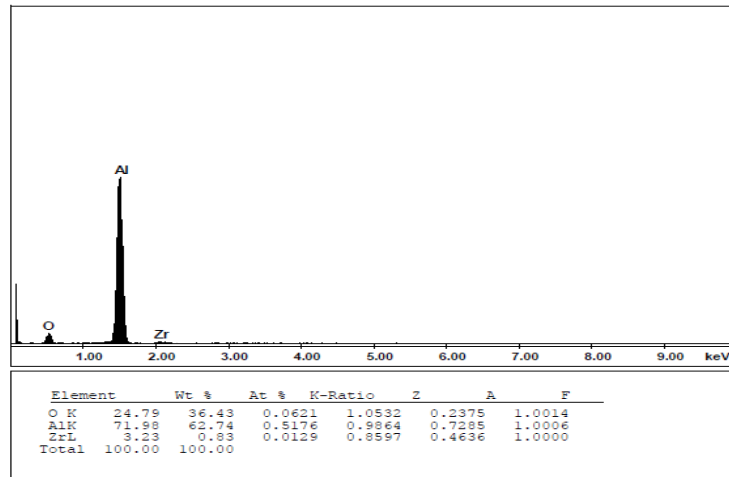


Fig. 18: EDAX of Al - (20-x) wt.-% Al<sub>2</sub>O<sub>3</sub> - (x) ZrO<sub>2</sub>, x= 4, composite sintered for 1 h at 470 °C in argon and prepared from powers milled at 7h.

### 3.2.3 Microhardness of sintered composites

Fig.19 shows microhardness of Al-20 wt.-% Al<sub>2</sub>O<sub>3</sub> prepared from powder milled for different milling times and sintered in argon atmosphere at 470 °C for 1 h. Microhardness of sintered composites increased with increasing milling time of starting powders [ Alizadeh, M et al 2011; Shehata, F et al 2009; Belhadjamida, A et al 1991; Hernández, J.L.R et al 2012]. This increase in microhardness is a consequence of fine Al<sub>2</sub>O<sub>3</sub> particles dispersion in Al matrix-compacts; and also due to crystal size refinement of starting powders after milling which led to increasing the sinterability and lowering the porosity. Before milling, the particle distribution isn't uniform and the distance between particles is so high, but increasing milling time causes break of big and brittle alumina powders, decreases the distance between particles and indent them into the ductile aluminum powders. This leads to increasing the sinterability and consequently the hardness of composites. The maximum value of microhardness of compacts processed after 7h milling and sintering at 470°C attains 979 MPa.

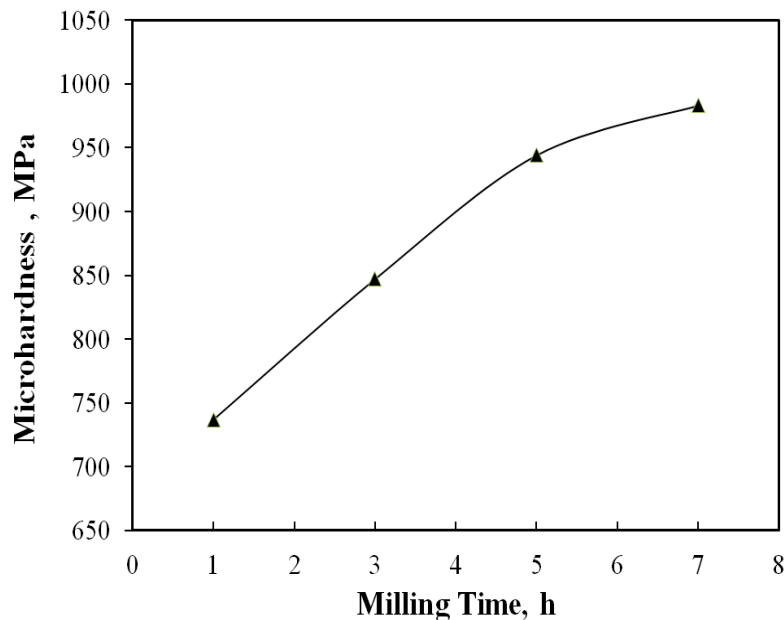


Fig. 19: Microhardness of Al-20 wt.-% Al<sub>2</sub>O<sub>3</sub> composites sintered for 1 h at 470°C prepared from powder versus milling time of starting powder.

It is well known that the hardness of ZrO<sub>2</sub> is higher than that of Al<sub>2</sub>O<sub>3</sub> and also it improves the microstructure through fining of the grains and limiting the grain growth. This leads to improving the hardness of the composite [ Francisco, A.T.G et al 2009; Zhao, Z et al 2005; Liu, G.J et al 1998; Tuan, W.H et al 2002]. Fig. 20 shows microhardness of Al - (20-x) wt.-% Al<sub>2</sub>O<sub>3</sub> - (x) ZrO<sub>2</sub>; x= 1, 2 & 4, sintered in argon atmosphere at 470 °C for 1 h and prepared from powders milled for 7 hrs. It is indicated

that the value of hardness increases with increasing zirconia's content reaching its maximum value with 4% zirconia (1070 MPa).

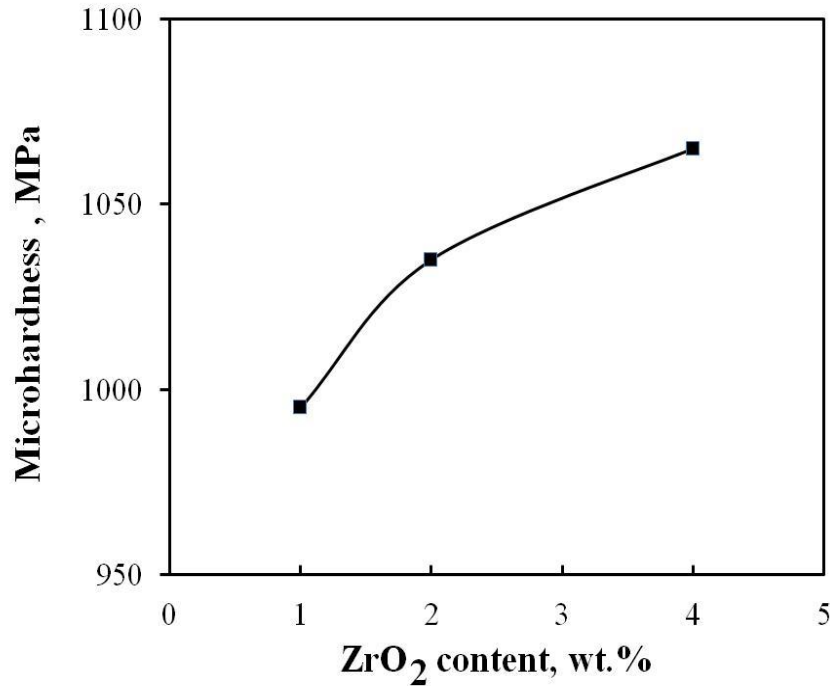


Fig. 20: Microhardness of Al - (20-x) wt.-% Al<sub>2</sub>O<sub>3</sub> - (x) ZrO<sub>2</sub>, x=1, 2 & 4, composites sintered for 1 h at 470 °C in argon and prepared from powers milled for 7h.

#### 4. Conclusion

The following remarks are concluded:

- Al - 20 wt.-% Al<sub>2</sub>O<sub>3</sub> nanocomposites have been successfully fabricated using mechanical alloying at different milling time (1, 3, 5 up to 7 h), in planetary ball mill. Another series of Al - (20-x) wt.-% Al<sub>2</sub>O<sub>3</sub> - (x) ZrO<sub>2</sub>; x= 1, 2 & 4 were fabricated after milling for 7h.
- Crystal size was found to be decreased while the lattice strain was found to be increased with increasing milling time due to distortion effect caused by dislocation in the lattice. The lattice parameters were found to stay constant during milling. With increasing milling time, severe plastic deformation brings about a deformed lattice with high density of dislocations

- Both morphology and particle size of nanocomposite powders were changed with increasing the milling time; the particle size has been decreased with increasing the time.
- Relative density of sintered nanocomposites was increased with increasing both milling time of the starting powders and sintering temperature. While, apparent porosity was found to be decreased.
- The hardness of sintered composites was affected by refining of grains and dispersion of Al<sub>2</sub>O<sub>3</sub> and/or ZrO<sub>2</sub> reinforcing particles in the composite with increasing milling time of starting powders. Microhardness of sintered bodies was found to be progressively increased with increasing of milling time of starting powders reaching 979 MPa in case of composite without ZrO<sub>2</sub> and 1070 MPa for composite with 4% ZrO<sub>2</sub>.

### **Acknowledgement**

Special thanks for late **Prof. Dr. Raghieba Abdel Wahab Esawey**, Prof. of Solid State Physics, National Research Center, Physics Division, Solid State Physics Department, for her supervision and fruitful discussion

### **5. References**

Alizadeh M, Aliabadi M.M, High-energy mechanical alloying (MA) of a micrometer-scaled W and TiC powder mixture was performed to prepare TiC/W nanocomposites, *Journal of Alloys and Compounds* 509, 4978-4986, (2011).

Aboraiia M.S., Abdalla G. A., Wasly H.S., Synthesis and Characterization of Al–Al<sub>2</sub>O<sub>3</sub> and Al/ (Al<sub>2</sub>O<sub>3</sub>-ZrO<sub>2</sub>) Nanocomposites Using High-Energy Milling, *Int. Journal of Engineering Research and Applications* ISSN : 2248-9622, Vol. 3, Issue 6, Nov-Dec, pp.1654-1663(2013).

Belhadjhamida A and German R.M, “Tungsten and tungsten alloys by powder metallurgy: a status review,” in *Tungsten and Tungsten Alloys Recent Advances*, A. Crowson and E. S. Chen, Eds., pp. 3–20, TMS, Warrendale, Pa, USA, 1991

Cullity B.D., *Elements of x-ray diffraction*, third ed., Prentice Hall, London, 2001.

Fogognolo J.B., Velasco F., Robert M.H., Torralba J.M., “Effect of mechanical alloying on the Morphology, microstructure and properties of aluminum matrix composite powder”, *Mat. Sci. Eng. A.*, Vol. 342, , 131-143(2003).

Francisco A.T.G., Ka'tia L.S, Trombini V, Juliano J.P., Jose´ A.R, Tomasi R, Eliria M.J.A.P. , Correlation between microstructure and mechanical properties of Al<sub>2</sub>O<sub>3</sub>/ZrO<sub>2</sub> nanocomposites, *Ceramics International* 35 741–745 (2009).

Guel I.G., Gallardo C.C., Ruiz D.C.M., Yoshida M.M., Rangel E.R., Sanchez R.M., J. Alloys Compd 483 173-177(2009).

Gubicza J., Kassem M., Ribarik G., Ungar T., The microstructure of mechanically alloyed Al–Mg determined by X-ray diffraction peak profile analysis, Mater. Sci. Eng., A 372 115–122(2004).

Hernández J. L. R, Cruz J.J. R, Pazdel V., Febles G, Alonso V. O. C, Sánchez R. M, Materials and Design 37 96–101(2012).

Hassan S.F., Gupta M., Effect of submicron size Al<sub>2</sub>O<sub>3</sub> particulates on microstructural and tensile properties of elemental Mg. J. Alloys Compd. 457, 244–250 (2008).

Hesabi Z.R, Simchi A and Reihani S.M.S, Structural evolution during mechanical milling of nanometric and micrometric Al<sub>2</sub>O<sub>3</sub> reinforced Al matrix composite. Materials Science and Engineering A 428 159–168 (2006).

Hanumanth G.S., Irons G.A., J. Mater. Sci. 28 2459-2465 (1993).

Hussain Z, Kit L.C, Properties and Spot Welding Behaviour of Copper-Alumina Composites through Ball Milling and Mechanical Alloying, Materials and Design 29 1311-1315 (2008).

Kaufman J.G., Properties of aluminum alloys; tensile, creep, and fatigue data at high and low temperatures, ASM International,( 2002).

Khakbiz M., Akhlaghi F., Synthesis and structural characterization of Al–B<sub>4</sub>C nano-composite powders by mechanical alloying, J. Alloys Compd., 479 334–34 (2009).

Korać M, Andić Z, Tasić M and Kamberović Ž, Sintering of Cu-Al<sub>2</sub>O<sub>3</sub> nano-composite powders produced by a thermochemical route J. Serb. Chem. Soc. 72 (11) 1115-1125 (2007).

Liu G.J., Qiu H.B., Todd R., Brook R.J., and Guo J.K., Processing and mechanical behavior of Al<sub>2</sub>O<sub>3</sub>/ZrO<sub>2</sub> nanocomposites, Materials Research Bulletin, Vol. 33, No. 2, pp. 281–288(1998).

Lu L., Zhang Y.F., Influence of process control agent on inter diffusion between Al and Mg during mechanical alloying, J. Alloys Compd. 290 279–283(1999).

Liu R.S., Shi W.C., Cheng Y.C., Huang C.Y., Crystal structures and peculiar magnetic properties of alpha- and gamma-(Al<sub>2</sub>O<sub>3</sub>) powders. *Mod. Phys. Lett. B* , 11, 1169–1174 (1997).

Lonnberg B, Characterization of milled Si<sub>3</sub>N<sub>4</sub> powder using X-ray peak, broadening and surface area analysis. *J. Mater. Sci.* 29 3224-3230 (1994).

Liu Y.Q., Cong H.T., Wang W., Sun C.H., Cheng H.M., *Mater. Sci. Eng. A* 505 151-156 (2009).

Miracle D.B., Metal matrix composites - from science to technological significance, *Compos. Sci. Technol.* 65 2526–2540 (2005).

Moustafa M.M.M., Omayma A.E., Abdelhameed A.W., *Open Journal of Metal*, 3 72-79 (2013) .

Maurice D, Courtney T.H., Modeling of mechanical alloying: part III. Applications of computational programs. *metall., Metallurgical and Materials Transaction*, 26A 2437 (1995).

Prabhu B., Suryanarayana C., An L., Vaidyanathan R., Synthesis and characterization of high volume fraction Al–Al<sub>2</sub>O<sub>3</sub> nanocomposite powders by high-energy milling, *Mater. Sci. Eng., A* 425 192–200 (2006).

Razavi S.S.T, Yazdani R.R, Salahi E, Rahimipour M.R., Kazemzade A. and Razavi M., *Materials and Energy Research Center* Vol. 22, No. 2, August 177(2009).

Rajković V, Erić O, Božić D, Mitkov M, Romhanji E , Characterization of Dispersion Strengthened Copper with 3wt% Al<sub>2</sub>O<sub>3</sub> by Mechanical Alloying, *Science of Sintering*, 36 205-211(2004).

Rosenberger M.R., Schvezov C.E., Forlerer E., *Wear* 259 590-601(2005).

Rajkovic V, Bozic D, Jovanovic M.T, Properties of copper matrix reinforced with nano- and micro-sized Al<sub>2</sub>O<sub>3</sub> particles. *Journal of Alloys and Compounds* 459 177-184(2008).

Rao P.G., Iwasa M., Tanaka T., Kondoh I., Inoue T., Preparation and mechanical properties of Al<sub>2</sub>O<sub>3</sub>–15wt.%ZrO<sub>2</sub> composites, *Scripta Materialia* 48 437–441(2003).

Suryanarayana C., Al-Aqeeli N., Mechanically alloyed nanocomposites, *Prog. Mater. Sci.* 58 383–502 (2013).

Shehata F., Fathy A., Abdelhameed M., Moustafa S. F., *Materials and Design* 30, 2756-2762, (2009).

Suryanarayana C, Mechanical alloying. Prog Mater Sci; vol.46, pp.1-184, (2001).

Tousi S.S.R, Rad R.Y, Salahi E, Mobasherpour I, Razavi M. Production of Al–20 wt. % Al<sub>2</sub>O<sub>3</sub> composite powder using high energy milling, powder Technology 192 346-351(2009).

Torralba J.M., da Costa C.E., Velasco F., P/M aluminum matrix composites: an overview, J. Mater. Processing Technol. 133 203–206 (2003).

Tuan W.H., Chen R.Z., Wang T.C., Cheng C.H., Kuo P.S., Mechanical properties of Al<sub>2</sub>O<sub>3</sub>/ZrO<sub>2</sub> composites. Journal of the European Ceramic Society 22 2827–2833 (2002).

Woo K., Lee H.B., Fabrication of Al alloy matrix composite reinforced with sub sieve-sized Al<sub>2</sub>O<sub>3</sub> particles by the in situ displacement reaction using high-energy ball-milled powder. Mater. Sci. Eng., A 449–451, 829–832 (2007).

Youssef K.M., Scattergood R.O., Murty K.L., Koch C.C., Scripta Materialia 54 251–256 (2006).

Zawrah M.F., Zayed H.A, Essawy A.S, Nassar A.H, Taha. M.A, Preparation by mechanical alloying, characterization and sintering of Cu–20 wt.% Al<sub>2</sub>O<sub>3</sub> nanocomposites, Materials and Design 46, 485–490 (2013).

Zebarjad S.A., Sajjadi S.A., Microstructure evaluation of Al–Al<sub>2</sub>O<sub>3</sub> composite produced by mechanical alloying method, Mater. Des. 27 684–688 (2006).

Zebarjad S.M., Sajjadi S.A., Dependency of physical and mechanical properties of mechanical alloyed Al–Al<sub>2</sub>O<sub>3</sub> composite on milling time, Mater. Des. 28 2113–2120 (2007).

Zhou F, Lee J, Lavernia E.J, Grain growth kinetics of a mechanically milled nanocrystalline Al. Scripta Mater. 44 2013-2017 (2001).

Zhou Y, Li Z.Q., Structural characterization of a mechanical alloyed Al–C mixture. J. Alloys Compd. 414 107-112 (2006).

Zhao Z, Zhang L, Jian Zheng J, Bai H, Zhang S, Xu B, Microstructures and mechanical properties of Al<sub>2</sub>O<sub>3</sub>/ZrO<sub>2</sub> composite produced by combustion synthesis, 1 Scripta Materialia 53 (2005) 995–1000.

## الملخص باللغة العربية

### تحضير وتوصيف بعض المتراكبات من لحمة فلزية مدعمة بأكسيد الالومنيوم والزركونيوم

محمود فرج زورة<sup>1</sup>، احمد جمال الدين مصطفى<sup>2</sup>، فردوس احمد سعدالله<sup>1</sup>، محمد يسرى حسان<sup>2</sup>  
محمد عبد العزيز طه<sup>1</sup>، محمود نصر الدين محمد<sup>1</sup>

١. قسم الكيمياء غير العضوية وقسم الجوامد المركز القومي للبحوث، 2. قسم الجوامد جامعة الأزهر

تم تحضير متراكبات نانومترية من لحمة فلزية مدعمة بأكسيد الالومنيوم وأكسيد الزركونيوم بطريقة التحضير الميكانيكي حتى زمن طحن ٧ ساعات. تم دراسة تأثير زمن الطحن على خواص المسحوق المحضر بواسطة نموذج حيود الأشعة السينية والميكروسكوب الإلكتروني النافذ وذلك للتأكد من النسب الكيميائية للمتراكبات الناتج ووجود أكثر من طور للمادة ودراسة حجم البلورات وأشكالها. تم بعد ذلك كبس المسحوق الناتج في صورة أقراص وأختصاعها لحرارات حرق عند ٣٠٠ و ٣٧٠ و ٤٧٠ درجة مئوية لمدة ساعة في وجود غاز الأرجون. تم دراسة الخواص الفيزيائية للعينات مثل الكثافة النسبية والمسامية الظاهرية بطريقة أرشميدس. كما تم عمل دراسة بالميكروسكوب الإلكتروني الماسح وتحليل طيفي بواسطة حيود الأشعة السينية للتأكد من نسب العناصر. كما تم عمل دراسة لخاصية الصلابة الميكانيكية للمتراكبات ومن خلال الدراسة وجد ان قيمة الصلابة تزداد بازدياد ساعات الطحن وتم تفسير النتائج. ووجد ان حجم الحبيبات قد وصل الى 20 نانومتر بعد زمن طحن ٧ ساعات مع ملاحظة وجود بعض التكتلات الحبيبية. ووجد ان توزيع حبيبات كلا من أكسيد الالومنيوم وأكسيد الزركونيوم في لحمة الالومنيوم يزيد بانتظام مع زيادة عدد ساعات الطحن. كما وجد ان الكثافة النسبية تزداد أيضا بازدياد عدد ساعات الطحن وحرارة الحرق.